

## Aerosol distributions and radiative forcing over the Asian Pacific region simulated by Spectral Radiation-Transport Model for Aerosol Species (SPRINTARS)

Toshihiko Takemura,<sup>1</sup> Teruyuki Nakajima,<sup>2</sup> Akiko Higurashi,<sup>3</sup> Sachio Ohta,<sup>4</sup> and Nobuo Sugimoto<sup>3</sup>

Received 25 November 2002; revised 20 February 2003; accepted 24 March 2003; published 6 August 2003.

[1] A three-dimensional aerosol transport-radiation model coupled with a general circulation model, Spectral Radiation-Transport Model for Aerosol Species (SPRINTARS), simulates atmospheric aerosol distributions and optical properties. The simulated results are compared with aerosol sampling and optical observations from ground, aircraft, and satellite acquired by intensive observation campaigns over east Asia in spring 2001. Temporal variations of the aerosol concentrations, optical thickness, and Ångström exponent are in good agreement between the simulation and observations. The midrange values of the Ångström exponent, even at the Asian dust storm events over the outflow regions, suggest that the contribution of the anthropogenic aerosol, such as carbonaceous and sulfate, to the total optical thickness is of an order comparable to that of the Asian dust. The radiative forcing by the aerosol direct and indirect effects is also calculated. The negative direct radiative forcing is simulated to be over  $-10 \text{ W m}^{-2}$  at the tropopause in the air mass during the large-scale dust storm, to which both anthropogenic aerosols and Asian dust contribute almost equivalently. The direct radiative forcing, however, largely depends on the cloud water content and the vertical profiles of aerosol and cloud. The simulation shows that not only sulfate and sea salt aerosols but also black carbon and soil dust aerosols, which absorb solar and thermal radiation, make strong negative radiative forcing by the direct effect at the surface, which may exceed the positive forcing by anthropogenic greenhouse gases over the east Asian region. *INDEX TERMS:* 0305 Atmospheric Composition and Structure: Aerosols and particles (0345, 4801); 0365 Atmospheric Composition and Structure: Troposphere—composition and chemistry; 0368 Atmospheric Composition and Structure: Troposphere—constituent transport and chemistry; 3359 Meteorology and Atmospheric Dynamics: Radiative processes; *KEYWORDS:* aerosol, global model, radiative forcing, ACE-Asia, APEX, dust

**Citation:** Takemura, T., T. Nakajima, A. Higurashi, S. Ohta, and N. Sugimoto, Aerosol distributions and radiative forcing over the Asian Pacific region simulated by Spectral Radiation-Transport Model for Aerosol Species (SPRINTARS), *J. Geophys. Res.*, 108(D23), 8659, doi:10.1029/2002JD003210, 2003.

### 1. Introduction

[2] Atmospheric aerosols have a harmful influence on the respiration system of man and animals so that the emission control of aerosols originating from industrial activities is being enforced mainly in developed nations. For instance, sulfate aerosols and sulfur dioxide in the atmosphere, which are one of the main origins of acid rain, tend to decrease by the introduction of low-sulfur fuel and desulfurizers. In Asian countries, however, the emission of anthropogenic

aerosols and their precursor gases is predicted to continue increasing for the next several decades with the recent rapid growth of the economy and population [*Intergovernmental Panel on Climate Change (IPCC)*, 2000]. The scale and frequency of Asian dust storms in springtime have also rapidly increased since 2000, which made visibility and the atmospheric environment worse in northern China, Korea, and Japan. The Asian dust storms were detected by satellite retrievals from the Total Ozone Mapping Spectrometer (TOMS) and the Sea-viewing Wide Field-of-view Sensor (SeaWiFS); it was found that the huge dust storms reached North America by crossing the North Pacific Ocean [*Takemura et al.*, 2002a; *Thulasiraman et al.*, 2002].

[3] The variation of spatial distributions of aerosol particles also causes a change in the earth's radiation budget through two effects. One is a direct effect in which aerosol particles scatter and absorb the solar and thermal radiation. The other is an indirect effect in which they alter the microphysical and optical properties of cloud droplets acting

<sup>1</sup>Research Institute for Applied Mechanics, Kyushu University, Fukuoka, Japan.

<sup>2</sup>Center for Climate System Research, University of Tokyo, Tokyo, Japan.

<sup>3</sup>National Institute for Environmental Studies, Tsukuba, Japan.

<sup>4</sup>Graduate School of Engineering, Hokkaido University, Sapporo, Japan.

as cloud condensation nuclei (CCN). Twomey [1974] indicated that an increase in aerosol particles causes an increase in the cloud droplet number concentration and a decrease in the cloud droplet size for a fixed liquid water content, leading to a high cloud albedo (the first indirect effect). Albrecht [1989] indicated that a reduction of the cloud droplet size results in an increase of the liquid water content by a decrease of precipitation efficiency (the second indirect effect). The confidence level of the aerosol radiative forcing estimated by the Intergovernmental Panel on Climate Change [IPCC, 2001] is, however, much lower than those of the greenhouse gases and ozone. The global mean radiative forcing due to anthropogenic aerosols was estimated to be  $-0.5 \text{ W m}^{-2}$  with an uncertainty factor of 2 for the direct effect and 0 to  $-2.0 \text{ W m}^{-2}$  without a plausible value for the first indirect effect by IPCC [2001]. The second indirect effect could not even be evaluated. One of the reasons for the uncertainty is in the difficulty of modeling for simulating global aerosol distributions because of the complex characteristics of aerosol particles such as various origins, short lifetime, complex chemical components, and various size distributions. In recent studies distributions of all the main tropospheric aerosol species have been simulated more precisely with the global models by comparing aerosol mass concentrations and optical properties with many ground-based and satellite observations [Chin et al., 2002; Takemura et al., 2002b]. In the Asian region, however, aerosol observations have been insufficient for validating aerosol models and understanding the aerosol effects on the climate system. The Asian atmospheric environment has been worsened rapidly by Asian dust and anthropogenic gases and aerosols in recent years.

[4] To break the insufficiency of the observational frequency and network on Asian atmospheric aerosols, two projects have been organized: APEX (Asian Atmospheric Particulate Environmental Change Studies) and ACE-Asia (Asian Pacific Regional Aerosol Characterization Experiment). APEX is a Japanese project to operate from 1999 to 2004; its purpose is to understand cloud-aerosol interaction and the change of the radiative budget by aerosols and clouds (T. Nakajima et al., Significance of direct and indirect radiative forcings of aerosols in the east China Sea region, submitted to *Journal of Geophysical Research*, 2003, hereinafter referred to as Nakajima et al., submitted manuscript, 2003). Intensive observation campaigns using ground-based, airborne, shipboard, and satellite instruments were carried out in December 2000 (APEX-E1) and April 2001 (APEX-E2) around Amami-Oshima ( $129.7^\circ\text{E}$ ,  $28.4^\circ\text{N}$ ). ACE-Asia was an international intensive observation project carried out off the coast of China, Japan, and Korea from March to May 2001 [Huebert et al., 2003]. In this study the three-dimensional distributions of aerosol mass concentrations and optical properties were simulated by the global aerosol model, SPRINTARS (Spectral Radiation-Transport Model for Aerosol Species), and compared with various observed data acquired by APEX and ACE-Asia in order to confirm the accuracy of the simulation and to analyze observed results over the east Asian region. Since SPRINTARS can simultaneously calculate both the direct and indirect aerosol radiative forcings, they are discussed for the Asian region. The model description is given in section 2. Section 3 shows the monthly mean

characteristics of the Asian dust and anthropogenic aerosol distributions in December 2000 (APEX-E1) and April 2001 (APEX-E2/ACE-Asia) simulated by SPRINTARS. The simulated aerosol mass concentrations and optical properties are also compared with the ground-based filter samplings and optical observations by satellite, aircraft, and lidar. In section 5 the aerosol radiative forcing calculated by SPRINTARS is discussed. Our conclusions are presented in section 6.

## 2. Model Description

[5] The three-dimensional global aerosol climate model, SPRINTARS, has been developed at the Center for Climate System Research (CCSR), University of Tokyo. The model simultaneously treats the main tropospheric aerosols, that is, carbonaceous (organic carbon (OC) and black carbon (BC)), sulfate, soil dust, and sea salt, and the precursor gases of sulfate, that is, sulfur dioxide ( $\text{SO}_2$ ) and dimethylsulfide (DMS). The aerosol transport processes include emission, advection, diffusion, sulfur chemistry, wet deposition, dry deposition, and gravitational settling. The model is driven by the atmospheric general circulation model (AGCM) of CCSR in common with the National Institute for Environmental Studies (NIES), Japan [Numaguti et al., 1995]; the radiation scheme in CCSR/NIES AGCM [Nakajima et al., 2000] is extended to the radiative process related with aerosol particles for SPRINTARS. The horizontal resolution of the triangular truncation is set at T42 (approximately  $2.8^\circ$  by  $2.8^\circ$  in latitude and longitude) and the vertical resolution at 11 layers (sigma level based on the surface pressure at 0.995, 0.980, 0.950, 0.900, 0.815, 0.679, 0.513, 0.348, 0.203, 0.092, and 0.021). The present study uses the National Centers for Environmental Prediction (NECP)/National Center for Atmospheric Research (NCAR) every 6-hour reanalysis data for nudging the wind, temperature, and specific humidity during the specific period. The detailed explanations for SPRINTARS are described by Takemura et al. [2000] for the aerosols transport processes and by Takemura et al. [2002b] for the revised transport processes and the radiative process.

[6] A few emission data for carbonaceous and  $\text{SO}_2$  are renewed for the 2000/2001 simulation. The anthropogenic  $\text{SO}_2$  emission flux is based on the Special Report on Emissions Scenarios (SRES) [IPCC, 2000]. It is divided into four regions of the world (OECD; eastern Europe and the former Soviet Union; Asia; Africa, Middle East, and Latin America); then the gridded emission pattern within each region follows the Global Emissions Inventory Activities (GEIA) database for  $\text{SO}_2$  [Benkovitz et al., 1996]. The carbonaceous aerosol emission fluxes are based on SRES for fossil fuel, biomass burning, and biofuel origins, but they are not included directly in the SRES data set. Therefore the carbonaceous aerosol emission inventory is made from the SRES  $\text{CO}_2$  emission, which is then scaled and gridded by the GEIA database for fossil fuel and biomass burning sources [Cooke and Wilson, 1996] and the original data for biofuel sources [Takemura et al., 2000]. The simulation also includes the  $\text{SO}_2$  emission from the large-scale continuous eruption of Miyakejima Island ( $139.5^\circ\text{E}$ ,  $34.1^\circ\text{N}$ ) with temporal variation, which is important for calculating the appropriate aerosol distribution in east Asia from 2000 to 2002.

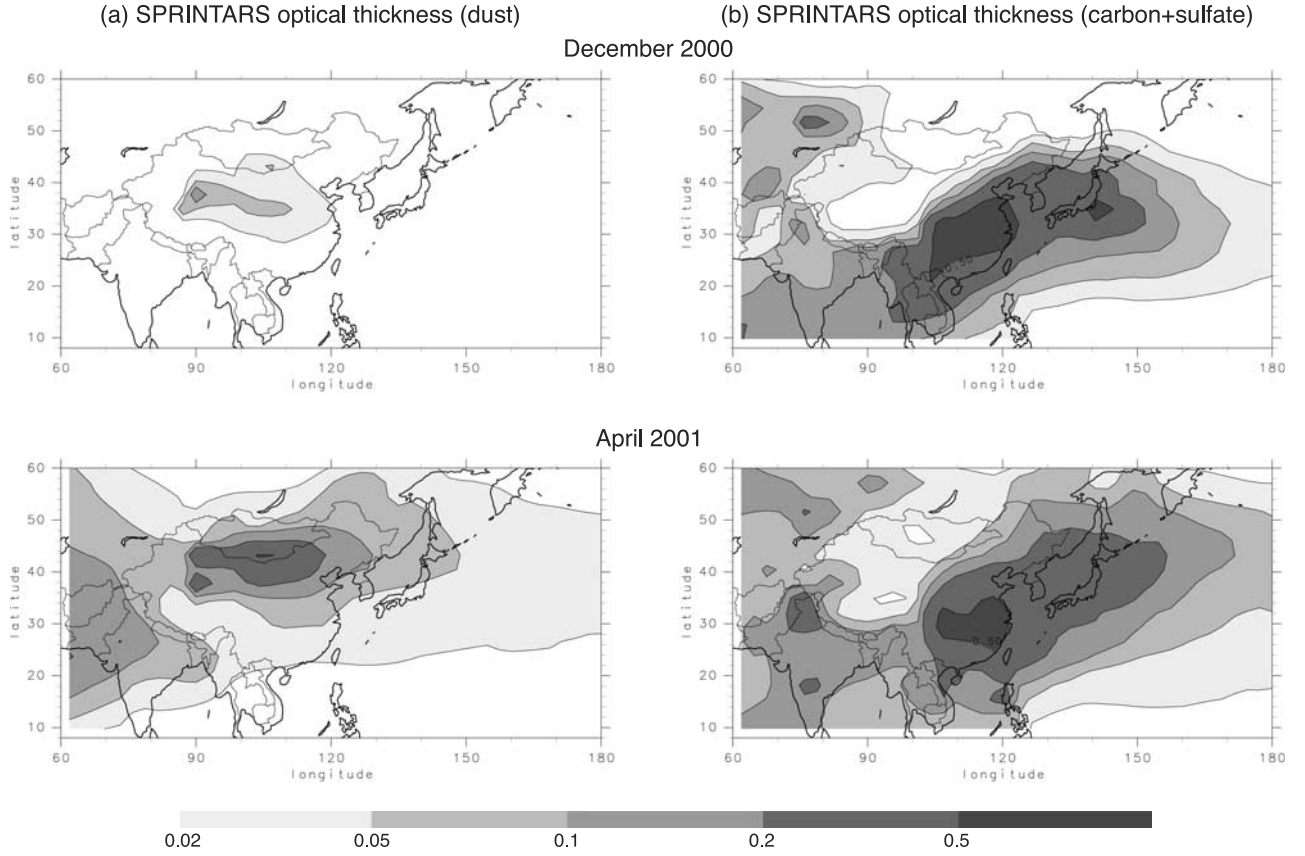


**Figure 1.** Monthly mean distributions of the optical thickness at  $0.55 \mu\text{m}$  for (a) soil dust aerosols and (b) carbonaceous plus sulfate aerosols in December 2000 and April 2001 simulated by SPRINTARS.

[7] The present study considers both the first and second aerosol indirect effects only for stratus cloud. The cloud droplet number concentration  $N_c$  is diagnosed referring to the observation by *Martin et al.* [1994]:

$$N_c = \frac{\varepsilon N_a N_m}{\varepsilon N_a + N_m}, \quad (1)$$

where  $N_a$  is the aerosol number concentration excluding soil dust aerosols, and  $\varepsilon$  and  $N_m$  are constants. The role of soil dust aerosols in CCN is poorly understood so that they are excluded from  $N_a$  in equation (1), though they may act as CCN if other hydrophilic aerosols are internally mixed with them. The Berry's parameterization is adapted to the precipitation rate  $P$ , which depends not only on cloud water mixing ratio  $l$ , but also on  $N_c$  [Berry, 1967]:

$$P = -\frac{dl}{dt} = \frac{\alpha \rho l^2}{\beta + \gamma \frac{N_c}{\rho l}}, \quad (2)$$

where  $t$  is time,  $\rho$  is the air density, and  $\alpha$ ,  $\beta$ , and  $\gamma$  are constants. If the function of the cloud droplet size distribution is fixed, its effective radius  $r_{\text{eff}}$  is decided as follows:

$$r_{\text{eff}} = k \left( \frac{3}{4\pi\rho_w N_c} \right)^{\frac{1}{3}}, \quad (3)$$

where  $\rho_w$  is the water density and  $k$  is an empirical constant. The indirect radiative forcing in this study is defined as the difference of the radiative budget between the simulations given the standard aerosol emission data set and the nonanthropogenic emission from east Asia.

### 3. Results and Discussion

#### 3.1. Simulated Distributions of Asian Aerosols

[8] Figure 1 shows the monthly mean distributions of the optical thickness at  $0.55 \mu\text{m}$  for soil dust aerosols and carbonaceous plus sulfate aerosols in December 2000 and April 2001 simulated by SPRINTARS. The Asian dust events are rarely observed in winter due to the high-pressure system over the source regions, which is consistent with only a small amount of dust emission from the Takla Makan Desert in December 2000 in the simulation. Anthropogenic aerosols originating from the east Asian continent and additionally from southeast Asia by biomass burning are transported to the east. The optical thickness of carbonaceous plus sulfate aerosols is over 0.5 around the source region. Therefore the observational data acquired by APEX-E1 is useful for analyzing anthropogenic aerosols without mixing of the Asian dust in east Asia. The simulation also indicates that the sulfate aerosol formed from the volcanic  $\text{SO}_2$  of the Miyakejima Island is a large contributor to air turbidity.

[9] In the spring, on the other hand, the dust events frequently occur because the developing cyclone passes

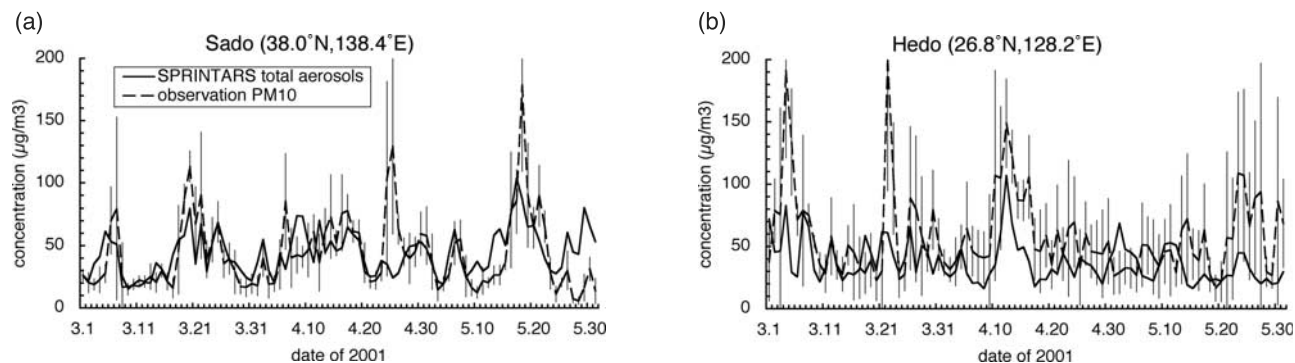


**Figure 2.** Comparison of the simulated total aerosol mass concentration (solid line) with the observed PM10 concentration (dashed line) in  $\mu\text{g m}^{-3}$  from March to May 2001 at (a) Sado (38.0°N, 138.4°E) and (b) Hedo (26.8°N, 128.2°E).

through desert areas every several days. The simulation suggests that the Gobi Desert is also a main dust source, where is east of the Takla Makan Desert, so that the Asian dust is easily transported to Korea, Japan, and the North Pacific. The large-scale Asian dust storm early in April 2001 was simulated to reach the west coast of North America crossing by the North Pacific Ocean by SPRINTARS, of which the temporal and spatial patterns are closely similar to the aerosol index retrieved from the TOMS observation [Takemura *et al.*, 2002a]. Anthropogenic aerosols are transported more northward in spring than in winter because cyclones often move to the east between 40° to 60°N, while the northwest wind is predominant in winter. Takemura *et al.* [2002a] indicated that a large amount of anthropogenic aerosols was transported to the North Pacific mixing with soil dust aerosols during the large-scale Asian dust storm early in April 2001, which was attributed to the developed cyclone. Figure 1b also shows that the optical thickness of anthropogenic aerosols reduces near the source region and that they diffuse further in spring than in winter. This is due to not only frequent passages of cyclones but also the instability of the atmosphere.

### 3.2. Comparisons With Observations

[10] There is a large volume of observational data regarding the aerosol mass and optical characteristics in the spring of 2001 acquired during APEX-E2 and ACE-Asia. Figure 2 shows comparisons between the simulated total aerosol

mass concentration and the particle matter concentration below the 10- $\mu\text{m}$  diameter (PM10) observed by the Acid Deposition and Oxidant Research Center (ADORC). Large particles, such as soil dust and sea salt aerosols, are main contributors to the PM10 concentration, so that the high PM10 concentration suggests the arrival of Asian dust in east Asia. The simulation represents the observed temporal variation well over the coast of the Japan Sea (Figure 2a). The dust storms arrived in early and the latter half of March, mid-April, and mid-May with the eastward migration of developed cyclones. At Okinawa Island, southwest of Japan, the high PM10 concentrations were observed during the same periods as the Japan Sea side (Figure 2b). This suggests that the aerosol concentration was high along the cold front, which was clearly shown by Takemura *et al.* [2002a]. The simulated total aerosol concentration is, however, underestimated because of the weak southward flow of Asian dust in Figure 2b, although the temporal variation is in reasonable agreement with the observation. It is also an interesting point that both the observation and simulation show much larger temporal variations of aerosol concentrations at Hedo than Sado because the location is near the east Asian continent that has various natural and anthropogenic aerosol sources.

[11] Figure 3 shows a time series of the simulated BC and  $\text{SO}_4^{2-}$  concentrations in comparison with the observation at Amami-Oshima acquired by APEX-E2 in April 2001. It is impossible to detect either of them from the PM10 or total

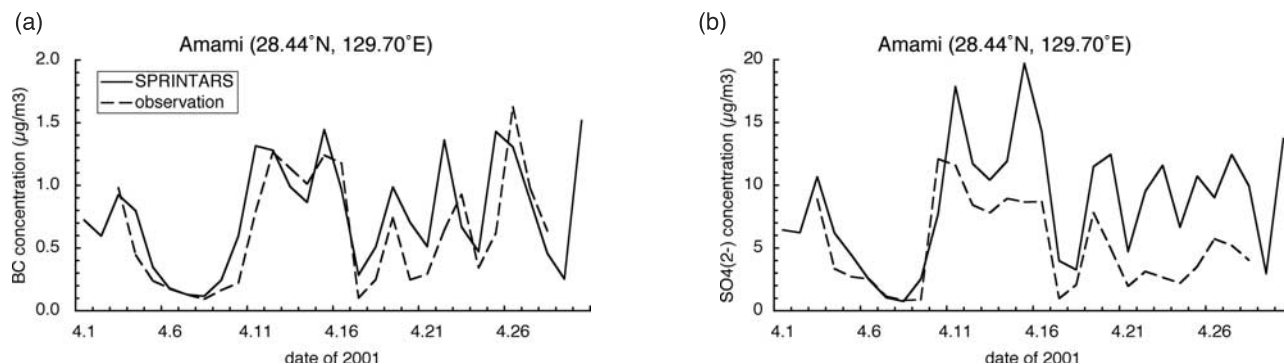


**Figure 3.** Comparison of the simulated mass concentration (solid line) with the observation (dashed line) for (a) BC and (b)  $\text{SO}_4^{2-}$  in  $\mu\text{g m}^{-3}$  in April 2001 at Amami-Oshima (28.4°N, 129.7°E).

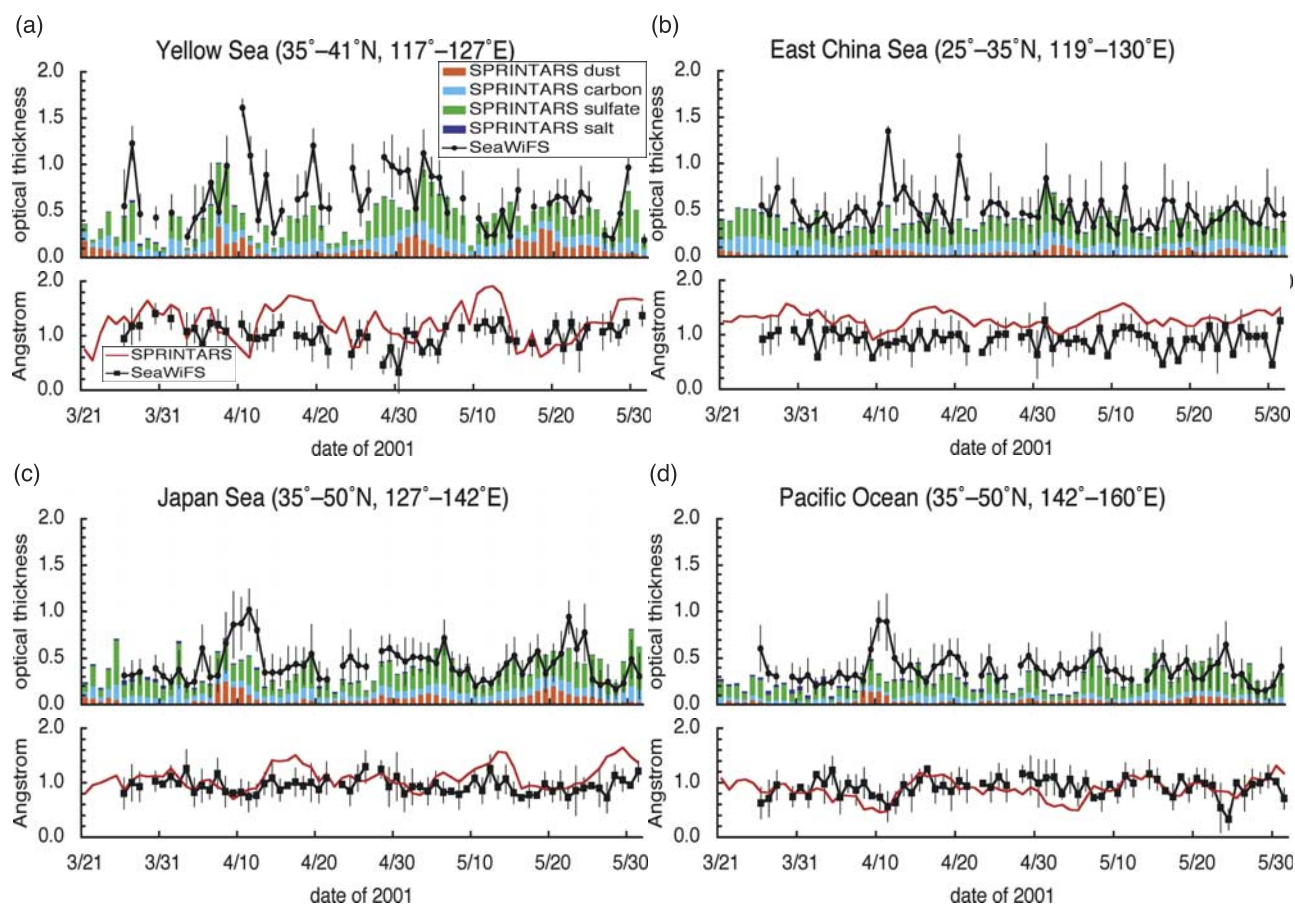


**Figure 4.** Time series of the simulated optical thickness for each aerosol component (column), simulated Ångström exponent (red line), SeaWiFS optical thickness (black line with dot), and SeaWiFS Ångström exponent (black line with square) from 21 March to 31 May 2001 over the (a) Yellow Sea (35°–41°N, 117°–127°E), (b) east China Sea (25°–35°N, 119°–130°E), (c) Japan Sea (35°–50°N, 127°–142°E), and (d) northwest Pacific Ocean (35°–50°N, 142°–160°E). Error bars in the SeaWiFS retrieval show the standard deviation in each target area.

aerosol concentrations, such as Figure 2, because the ratio of their mass concentrations to total aerosols is much lower than that of soil dust aerosols due to their small particle size. Both the BC and  $\text{SO}_4^{2-}$  concentrations are in good agreement between the simulation and observation. The temporal variation is closely similar to that of the total aerosol concentration shown in Figure 2b. The high BC and  $\text{SO}_4^{2-}$  concentrations in mid-April according to the high total aerosol concentration suggest the arrival of the air mass including both anthropogenic aerosols and Asian dust over Japan although their source regions are quite different.

[12] It is important to compare the simulated aerosol optical properties with observations from satellite, ground, and aircraft because they directly relate to the estimation of the aerosol direct radiative forcing. In Figure 4, the regional daily mean values of the simulated aerosol optical thickness and Ångström exponent are compared with the SeaWiFS retrieval in spring 2001 [Higurashi and Nakajima, 2002]. The Ångström exponent is an aerosol size index which is defined as the log-slope exponent of the spectral optical thickness between two wavelengths. The observation by Aerosol Robotic Network (AERONET) indicates the representative values of the Ångström exponent to be from 1.2 to

2.5 in urban areas and from 0.1 to 0.9 in desert areas [Dubovik *et al.*, 2002]. The simulated optical thickness is shown for each aerosol component. The temporal variations of the simulation and observation are in reasonable agreement for both the optical thickness and Ångström exponent, although the regional mean values of the SeaWiFS aerosol optical thickness tend to be greater than the simulated values because the SeaWiFS data can be retrieved only under clear-sky conditions and because it is difficult to pick up the pixel data only under clear-sky conditions from the simulated results. The difference between the simulated and SeaWiFS Ångström exponents over the east China Sea might occur not only by the simulated weak southward outflow of Asian dust as shown in Figure 2b but also by the peculiar ocean color due to the Asian dust outflow from the rivers. The mean biases of the simulated optical thickness to the SeaWiFS one are 35, 28, 28, and 29% over Yellow Sea, east China Sea, Japan Sea, and northwest Pacific Ocean, respectively. The mean standard deviations of the biases of the Ångström exponent between them are 0.22, 0.20, 0.17, 0.15, respectively. The agreement between the simulated and observed Ångström exponent around 10 April when the large-scale Asian dust storm happened suggests that the

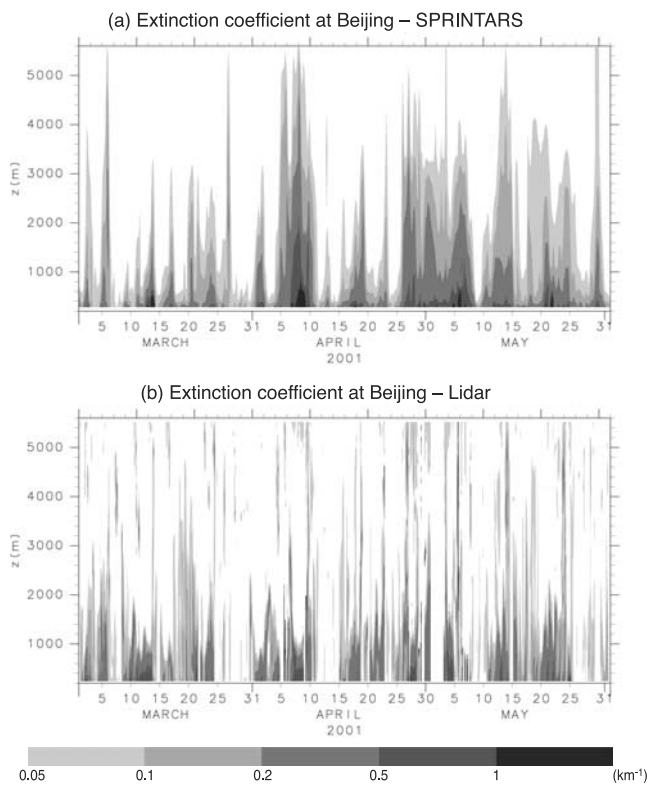


**Figure 5.** Time series of the vertical profiles of the aerosol extinction coefficient (a) simulated by SPRINTARS and (b) retrieved from the lidar observation in  $\text{km}^{-1}$  from March to May 2001 at Beijing, China.

ratio of the optical thickness of anthropogenic aerosols to that of soil dust aerosols is simulated well by SPRINTARS, which is clearly shown by the comparisons over the Japan Sea and northwest Pacific Ocean (Figures 4c and 4d). The simulation indicates that the contribution of anthropogenic aerosols to the total optical thickness is the same order of magnitude or greater than that of dust particles even during the dust events in the outflow regions.

[13] It is necessary to properly calculate not only the horizontal distribution but also the vertical profiles because the aerosol direct radiative forcing depends much on the relative altitude between aerosol and cloud layers, which will be discussed in the next section. Figure 5 shows the time series of the simulated vertical profiles of the aerosol extinction coefficient with the lidar observation at Beijing, China, several hundreds kilometer away from the Gobi Desert [Shimizu *et al.*, 2003]. The simulation reproduces well the high extinction coefficient in mid-March, early April, the end of April to early May, and in mid-May, all of which show the Asian dust events, though the lidar data cannot be sometimes retrieved due to vast dust loadings. Aerosol particles usually concentrate below 1.5 km, while the extinction coefficient is high also above 1.5 km during the arrival of the large-scale Asian dust storms.

[14] The vertical profiles of aerosol optical properties were also measured by the C-130 flights in ACE-Asia [Anderson *et al.*, 2003]. Figure 6 shows the comparison of the simulated aerosol extinction, Ångström exponent, and single scattering albedo with the two characteristic C-130

observations. To analyze the Ångström exponent makes distinction between soil dust and anthropogenic aerosols possible as indicated in Figure 4. In Figure 6a, the observational result shows that anthropogenic aerosols are prominent below 2 km as suggested by the large Ångström exponent value, while the main contributor to the extinction is found to be soil dust aerosols above 2 km. On the other hand, the observed Ångström exponent is rather homogeneous in Figure 6b. These characteristics of the vertical profiles are represented well by SPRINTARS.

#### 4. Direct and Indirect Radiative Forcings

[15] In the previous section, it was shown that SPRINTARS reproduces the aerosol concentration, optical thickness, and Ångström exponent in the Asian region in detail in spite of the coarse grid of the global model. The simulated aerosol radiative forcing is then discussed to consider the effect of aerosol particles on the climate system. Figures 7a to 7e show the daily mean distributions of the simulated aerosol optical properties on 10 April 2001. The optical thickness is large along the cold front over the Japan Sea due to the transportation of the large-scale Asian dust storm; the outflow of anthropogenic carbonaceous and sulfate aerosols from the southern coastal region of China also causes serious air pollution. The Ångström exponent is calculated to be small over the northern Chinese region as caused by Asian dust, while it is large over southeast Asia due to biomass burning mainly by agricultural activities. It takes intermediate values around 1.0 off the east Asian continent because Asian dust and anthropogenic aerosols are intermingled as discussed in the previous section. The simulated single scattering albedo is above 0.9 over almost all regions, except for southeast Asia and India because of the relatively high BC emission. The imaginary part of the refractive index of soil dust aerosols is revised to 0.002 at the visible wavelength in this study from 0.008 which is based on the old World Meteorological Organization recommendation [World Climate Research, 1983] because the simulated single scattering albedo by the previous version of SPRINTARS is much lower than the retrieved data from the AERONET [Takemura *et al.*, 2002b]. This revision results in good agreement between the simulated and observed single scattering albedo even in the dust layer as shown in Figure 6a.

[16] The simulated direct radiative forcing under a clear-sky condition shows strong negative forcing over the large optical thickness region, while it is positive north of 50°N due to the high surface albedo at the tropopause (Figure 7d). The daily mean value of the direct radiative forcing is calculated in excess of  $-10 \text{ W m}^{-2}$  along the coast of the east Asian continent. The contribution of anthropogenic aerosols to this large negative direct radiative forcing is 30 to 70% in the simulation. Under the whole-sky condition, which includes overcast areas, the direct radiative forcing is also positive over a part of the Pacific Ocean (Figure 7e). It is supposed that this is caused by absorbing strongly the multiple-scattered radiation of Asian dust and BC enhanced by the presence of low clouds. Figure 7f shows the simulated vertical distributions of the soil dust concentration and cloud water content along 152°E. It indicates that the Asian dust transport at an altitude between

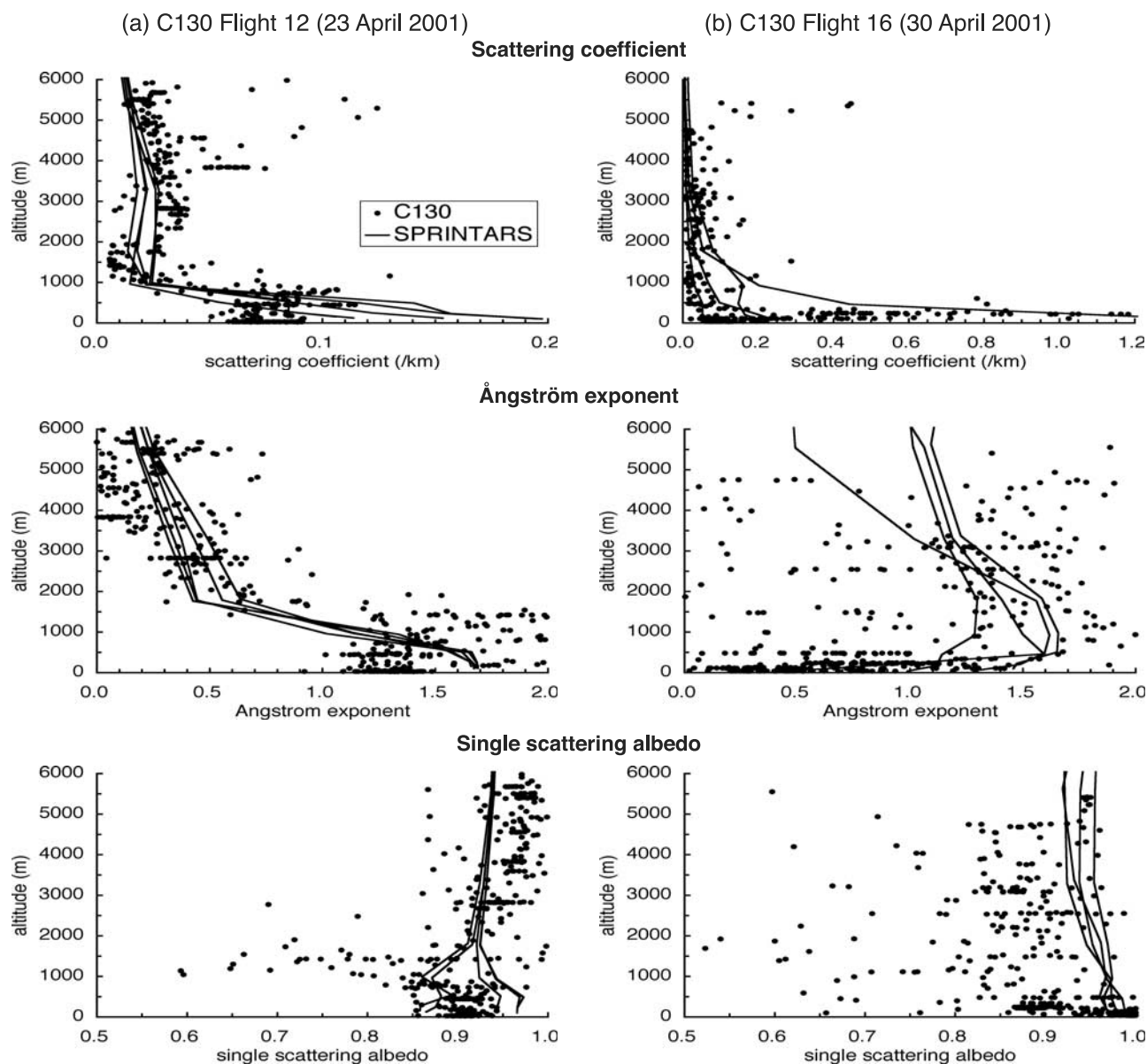


**Figure 6.** Comparison of the vertical profiles between the simulated (line) and C-130 flight (dot) aerosol scattering coefficient in  $\text{km}^{-1}$  (upper figure), Ångström exponent (middle figure), and single scattering albedo (bottom figure) over the (a) western Japan on 23 April and (b) southwestern Japan on 30 April 2001. The shown data are 2-hour mean values for the simulation and 1-minute mean for the observation. Both the simulated and observed extinction coefficient and single scattering albedo are at  $0.55 \mu\text{m}$ .

1 and 3 km and the low-level clouds below 1 km make strong positive forcing above the middle troposphere between  $40^\circ\text{N}$  and  $50^\circ\text{N}$ . The importance of the relative altitude of aerosol and cloud layers for aerosol direct radiative forcing was pointed out for the general condition [Haywood and Ramaswamy, 1998; Liao and Seinfeld, 1998; Takemura et al., 2002b].

[17] Table 1 shows monthly regional mean values of the direct radiative forcing for each aerosol component from  $90^\circ\text{E}$  to  $152^\circ\text{E}$  and from  $15^\circ\text{N}$  to  $52^\circ\text{N}$  in April 2001. As mentioned above, it is much different under clear- and whole-sky conditions, especially for carbonaceous aerosols which have negative and positive forcings at the tropopause,

respectively. It is characteristic of soil dust aerosols to take a large positive forcing at longwave radiation, so that the negative forcing at shortwave radiation is largely cancelled. The sulfate negative forcing at the tropopause is about three times as large as that of the global mean estimated by IPCC [2001] and Takemura et al. [2002b], which indicates that anthropogenic aerosols severely affect the radiation budget over east Asia. The simulation also shows that the difference of the radiative forcings between the tropopause and surface is large for aerosol particles absorbing the radiation, such as carbonaceous and soil dust aerosols. It is difficult to estimate an uncertainty of the simulated direct radiative forcing because it is related with a lot of aerosol optical

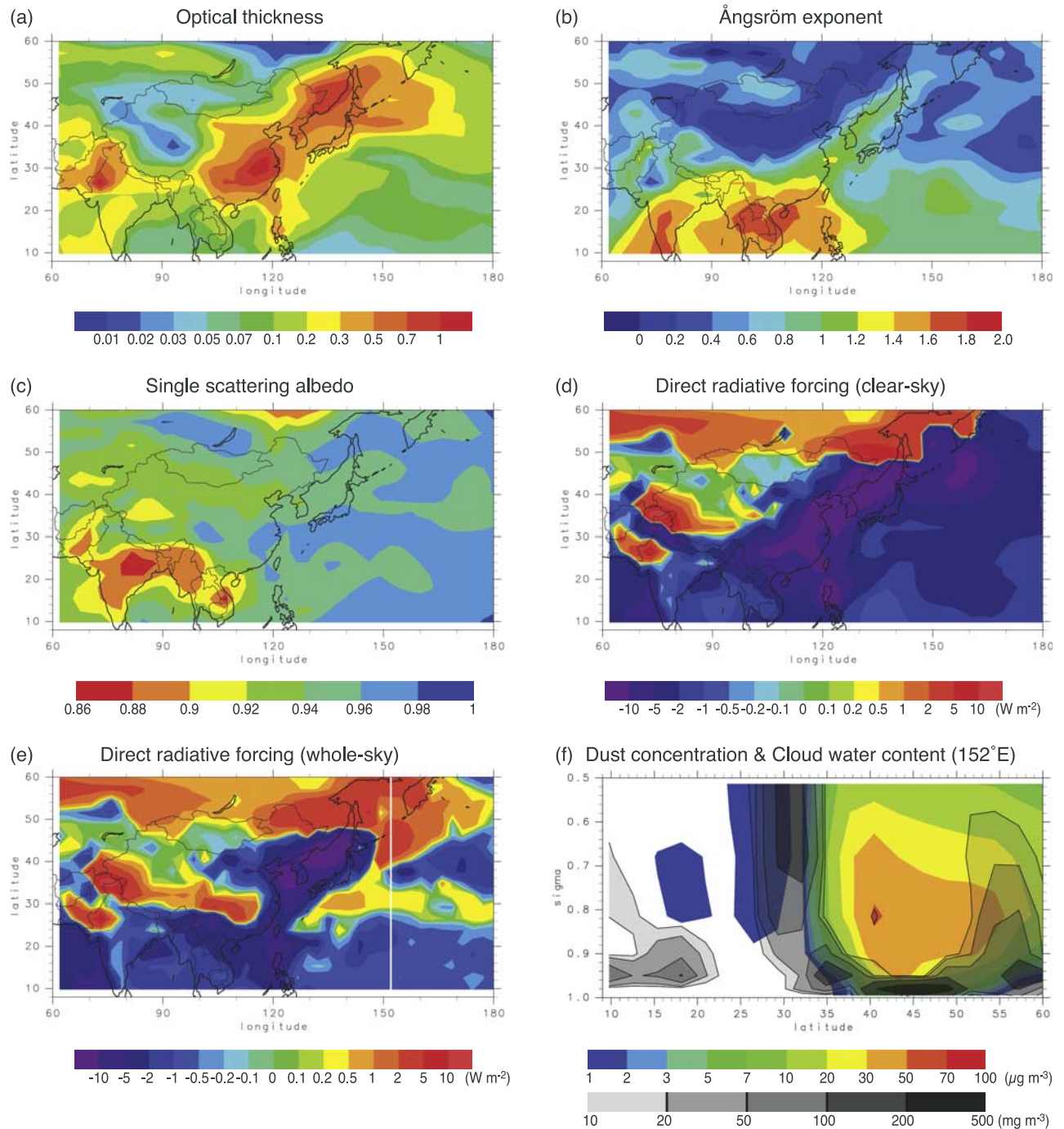


**Figure 7.** Daily mean distributions on 10 April 2001 of the simulated aerosol (a) optical thickness at  $0.55 \mu\text{m}$ , (b) Ångström exponent, (c) single scattering albedo at  $0.55 \mu\text{m}$ , direct radiative forcing under the (d) clear-sky condition and (e) whole-sky condition at the tropopause in  $\text{W m}^{-2}$ , and (f) vertical distributions of the soil dust mass concentration in  $\mu\text{g m}^{-3}$  (color) and cloud water content in  $\text{mg m}^{-3}$  (gray) along  $152^\circ\text{E}$ . The white line in Figure 7e shows  $152^\circ\text{E}$ .

parameters with wavelength dependence. If it must be estimated, it is about 30% in consideration of the bias between the simulated and observed aerosol optical thickness in Figure 4.

[18] The cloud-aerosol interaction is calculated using equations (1) to (3) derived from a quasi-empirical relationship. It is supposed that the interaction effectively occurs

over the east Asian region because of large concentrations both of aerosol particles and cloud droplets [Nakajima *et al.*, 2001]. Figure 8a shows the simulated cloud effective radius at a sigma level of 0.9, that is, an altitude about 1 km on a monthly average in April 2001. It takes small values between 8 and  $12 \mu\text{m}$  over eastern China, Korea, and Japan where the outflow of anthropogenic aerosols is strong. This is consist-

**Table 1.** Monthly and Regional Mean Values of the Simulated Direct Radiative Forcing for Each Aerosol Component From 15°N to 52°N and From 90°E to 152°E in April 2001 Under Clear- and Whole-Sky Conditions at the Tropopause and Surface in  $W m^{-2}$

	Tropopause			Surface		
	SW	LW	Total	SW	LW	Total
	<i>Clear Sky</i>					
BC + OC	-0.83	+0.03	-0.80	-4.57	+0.19	-4.38
Sulfate	-2.64	+0.08	-2.56	-2.64	+0.47	-2.17
Soil dust	-0.63	+0.44	-0.19	-1.93	+0.86	-1.07
Sea salt	-0.35	+0.01	-0.35	-0.36	+0.04	-0.32
	<i>Whole Sky</i>					
BC + OC	+0.11	+0.02	+0.13	-3.38	+0.12	-3.26
Sulfate	-1.35	+0.04	-1.31	-1.37	+0.27	-1.10
Soil dust	-0.32	+0.31	-0.02	-1.57	+0.64	-0.93
Sea salt	-0.23	+0.01	-0.23	-0.24	+0.02	-0.22

(SW = shortwave radiation, LW = longwave radiation.)

ent with the satellite retrievals from the National Oceanic and Atmospheric Administration Advanced Very High Resolution Radiometer (AVHRR) [Kawamoto *et al.*, 2001]. The negative radiative forcing of the aerosol first plus second indirect effects is also simulated to be strong in this area (Figure 8b). The monthly mean value of the calculated indirect radiative forcing in April 2001 is  $-1.8 W m^{-2}$  on a regional average of east Asia ( $101^{\circ}$ – $152^{\circ}E$ ,  $15^{\circ}$ – $52^{\circ}N$ ), which is as large as the estimation of the global mean for only the first indirect effect by IPCC [2001].

## 5. Conclusions

[19] A three-dimensional aerosol transport-radiation model, SPRINTARS, calculated aerosol distributions over the Asian Pacific region, and then the simulated results were compared with observed aerosol concentrations and various optical properties from ground, aircraft, and satellite acquired by the intensive observations of ACE-Asia and APEX in spring 2001. These comparisons confirmed that SPRINTARS successfully simulated temporal variations of aerosol parameters quantitatively. It was indicated by the simulation that air masses with the mixed state of Asian dust and anthropogenic aerosols are transported from the east

Asian continent to the Pacific region in springtime, which was also suggested by the midrange value of the Ångström exponent from the satellite retrieval. SPRINTARS also pointed out that the high concentrations of Asian dust and anthropogenic aerosols make a strong negative radiative forcing by the direct effect except for the areas of high surface albedo and low-level clouds. It was shown that the aerosol direct radiative forcing over the east Asian region is three times as large as the estimations of the global mean value by IPCC [2001].

[20] The quasi-empirical relationship of the number concentrations between aerosol particles and cloud droplets was adapted for calculating the aerosol indirect effect in this study. Many researchers are studying the cloud-aerosol interaction with various approaches. Khain *et al.* [2000] developed the detailed cloud microphysical model which can treat the cloud condensation and growth processes with the bin method. The APEX project is also continuing to analyze the cloud-aerosol interaction from the standpoint of the radiative and microphysical processes with ground, aircraft, and satellite observations and modeling studies (Nakajima *et al.*, submitted manuscript, 2003). It is important to construct an available parameterization in global models using knowledge from the above studies in more detail than equations (1) to (3).

[21] There are few past studies on considering fully the climate response to aerosols with aerosol transport models. Miller and Tegen [1998] discussed changes of the wind, surface temperature, precipitation, and surface heat flux with an AGCM including the prescribed three-dimensional distribution of soil dust aerosols. It is necessary to extend such a study to other aerosol species in order to advance climate change studies, especially for the Asian region because both soil dust and anthropogenic aerosols are intermingled at high concentration as shown in this study and because the anthropogenic pollutants emission is predicted to continue increasing for the next several decades in the east Asian continent due to rapid economic growth [IPCC, 2000]. SPRINTARS already has the potential of analyzing changes of the meteorological field by aerosol scattering and absorption of radiation because it is completely coupled with the AGCM. This is one of the near future studies for us.

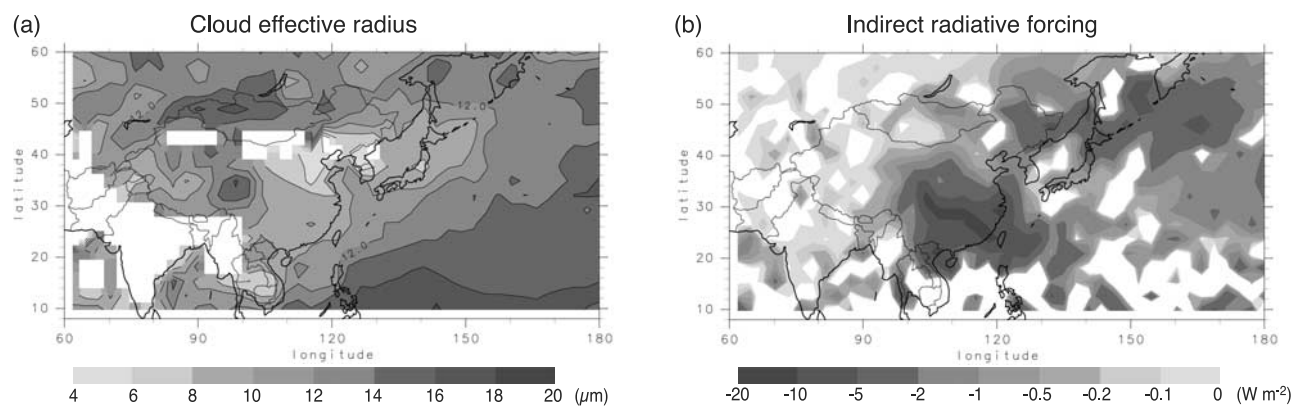


**Figure 8.** Monthly mean distributions of the simulated (a) cloud effective radius in  $\mu m$  and (b) aerosol indirect radiative forcing in  $W m^{-2}$  in April 2001.

[22] **Acknowledgments.** We thank the contributors to the development of the CCSR/NIES AGCM, A. Numaguti of Hokkaido University, who passed away in 2001, and K. Suzuki of the University of Tokyo for an idea of the parameterization of the cloud-aerosol interaction, the ADORC for providing the measured PM10 data, and T. L. Anderson and S. J. Masonis for analyzing data acquired from C-130 flights. This study is partly supported by the APEX project of the Core Research for Evaluational Science and Technology of the Japan Science and Technology Corporation.

## References

- Albrecht, B. A., Aerosols, cloud microphysics, and fractional cloudiness, *Science*, **245**, 1227–1230, 1989.
- Anderson, T., S. J. Masonis, D. S. Covert, N. Ahlquist, S. Howell, A. D. Clarke, and C. McNaughton, Variability of aerosol optical properties derived from in situ aircraft measurements during ACE-Asia, *J. Geophys. Res.*, **108**, doi:10.1029/2002JD003247, in press, 2003.
- Benkovitz, C. M., M. T. Scholtz, J. Pacyna, L. Tarrasón, J. Dignon, E. C. Voldner, P. A. Spiro, J. A. Logan, and T. E. Graedel, Global gridded inventories of anthropogenic emissions of sulfur and nitrogen, *J. Geophys. Res.*, **101**, 29,239–29,253, 1996.
- Berry, E. X., Cloud droplet growth by collection, *J. Atmos. Sci.*, **24**, 688–701, 1967.
- Chin, M., P. Ginoux, S. Kinne, O. Torres, B. N. Holben, B. N. Duncan, R. V. Martin, J. A. Logan, A. Higurashi, and T. Nakajima, Tropospheric aerosol optical thickness from the GOCART model and comparisons with satellite and sun photometer measurements, *J. Atmos. Sci.*, **59**, 461–483, 2002.
- Cooke, W. F., and J. J. N. Wilson, A global black carbon aerosol model, *J. Geophys. Res.*, **101**, 19,395–19,409, 1996.
- Dubovik, O., B. N. Holben, T. F. Eck, A. Smirnov, Y. J. Kaufman, M. D. King, D. Tanré, and I. Slutsker, Variability of absorption and optical properties of key aerosol types observed in worldwide locations, *J. Atmos. Sci.*, **59**, 590–608, 2002.
- Haywood, J. M., and V. Ramaswamy, Global sensitivity studies of the direct radiative forcing due to anthropogenic sulfate and black carbon aerosols, *J. Geophys. Res.*, **103**, 6043–6058, 1998.
- Higurashi, A., and T. Nakajima, Detection of aerosol types over the east China Sea near Japan from four-channel satellite data, *Geophys. Res. Lett.*, **29**(17), 1836, doi:10.1029/2002GL015357, 2002.
- Huebert, B., T. Bates, P. Russell, G. Shi, Y. J. Kim, and K. Kawamura, An overview of ACE-Asia: Strategies for quantifying the relationships between Asian aerosols and their climatic impacts, *J. Geophys. Res.*, **108**, doi:10.1029/2003JD003550, in press, 2003.
- Intergovernmental Panel on Climate Change (IPCC), *Special Reports on Emissions Scenarios*, edited by N. Nakicenovic and R. Swart, 612 pp., Cambridge Univ. Press, New York, 2000.
- Intergovernmental Panel on Climate Change (IPCC), *Climate Change 2001: The Scientific Basis*, edited by J. T. Houghton et al., 896 pp., Cambridge Univ. Press, New York, 2001.
- Kawamoto, K., T. Nakajima, and T. Y. Nakajima, A global determination of cloud microphysics with AVHRR remote sensing, *J. Clim.*, **14**, 2054–2068, 2001.
- Khain, A. P., M. Ovchinnikov, M. Pinsky, A. Pokrovsky, and H. Krugliak, Note on the state-of-the-art numerical modeling of cloud microphysics, *Atmos. Res.*, **55**, 159–224, 2000.
- Liao, H., and J. H. Seinfeld, Effects of clouds on direct aerosol radiative forcing of climate, *J. Geophys. Res.*, **103**, 3781–3788, 1998.
- Martin, G. M., D. W. Johnson, and A. Spice, The measurement and parameterization of effective radius of droplets in warm stratocumulus clouds, *J. Atmos. Sci.*, **51**, 1823–1842, 1994.
- Miller, R. L., and I. Tegen, Climate response to soil dust aerosols, *J. Clim.*, **11**, 3247–3267, 1998.
- Nakajima, T., M. Tsukamoto, Y. Tsushima, A. Numaguti, and T. Kimura, Modeling of the radiative process in an atmospheric general circulation model, *Appl. Opt.*, **39**, 4869–4878, 2000.
- Nakajima, T., A. Higurashi, K. Kawamoto, and J. E. Penner, A possible correlation between satellite-derived cloud and aerosol microphysical parameter, *Geophys. Res. Lett.*, **28**, 1171–1174, 2001.
- Numaguti, A., M. Takahashi, T. Nakajima, and A. Sumi, Development of an atmospheric general circulation model, in *Climate System Dynamics and Modeling*, edited by T. Matsuno, pp. 1–27, Cent. for Clim. Sys. Res., Univ. of Tokyo, Tokyo, 1995.
- Shimizu, A., N. Sugimoto, I. Matsui, K. Arai, I. Uno, T. Murayama, N. Kagawa, K. Aoki, A. Uchiyama, and A. Yamazaki, Continuous observations of Asian dust and other aerosols by polarization lidars in China and Japan during ACE-Asia, *J. Geophys. Res.*, **108**, doi:10.1029/2002JD003253, in press, 2003.
- Takemura, T., H. Okamoto, Y. Maruyama, A. Numaguti, A. Higurashi, and T. Nakajima, Global three-dimensional simulation of aerosol optical thickness distribution of various origins, *J. Geophys. Res.*, **105**, 17,853–17,873, 2000.
- Takemura, T., I. Uno, T. Nakajima, A. Higurashi, and I. Sano, Modeling study of long-range transport of Asian dust and anthropogenic aerosols from east Asia, *Geophys. Res. Lett.*, **29**(24), 2158, doi:10.1029/2002GL016251, 2002a.
- Takemura, T., T. Nakajima, O. Dubovik, B. N. Holben, and S. Kinne, Single scattering albedo and radiative forcing of various aerosol species with a global three-dimensional model, *J. Clim.*, **15**, 333–352, 2002b.
- Thulasiraman, S., N. T. O'Neill, A. Royer, B. N. Holben, D. L. Westphal, and L. J. B. McArthur, Sunphotometric observations of the 2001 Asian dust storm over Canada and U.S., *Geophys. Res. Lett.*, **29**(8), doi:10.1029/2001GL014188, 2002.
- Twomey, S., Pollution and the planetary albedo, *Atmos. Environ.*, **8**, 1251–1256, 1974.
- World Climate Research, *Report of the Experts Meeting on Aerosols and Their Climatic Effects, Rep. WCP-55*, edited by A. Deepak and H. E. Gerber, 107 pp., World Meteorol. Org., Geneva, 1983.

A. Higurashi and N. Sugimoto, National Institute for Environmental Studies, 16-2 Onogawa, Tsukuba, Ibaraki 305-8506, Japan. (hakiko@nies.go.jp; nsugimot@nies.go.jp)

T. Nakajima, Center for Climate System Research, University of Tokyo, 4-6-1 Komaba, Meguro-ku, Tokyo 153-8904, Japan. (teruyuki@ccsr.u-tokyo.ac.jp)

S. Ohta, Graduate School of Engineering, Hokkaido University, Kita 13 Nishi 8, Kita-ku, Sapporo 060-8628, Japan. (ohta@eng.hokudai.ac.jp)

T. Takemura, Research Institute for Applied Mechanics, Kyushu University, 6-1 Kasuga-koen, Kasuga, Fukuoka 816-8580, Japan. (toshi@riam.kyushu-u.ac.jp)